HER2^{YVMA} drives rapid development of adenosquamous lung tumors in mice that are sensitive to BIBW2992 and rapamycin combination therapy

Samanthi A. Perera[a,b], Danan Li[a,b], Takeshi Shimamura[a], Maria G. Raso[c], Hongbin Ji[d], Liang Chen[a,b], Christa L. Borgman[a], Sara Zaghlul[a], Kathleen A. Brandstetter[a], Shigeto Kubo[e], Masaya Takahashi[e], Lucian R. Chirieac[f], Robert F. Padera[f], Roderick T. Bronson[g], Geoffrey I. Shapiro[a], Heidi Greulich[a,h], Matthew Meyerson[a,h], Ulrich Guertler[i], Pilar Garin Chesa[i], Flavio Solca[i], Ignacio I. Wistuba[c,j], and Kwok-Kin Wong[a,b,1]

[a]Department of Medical Oncology, Dana–Farber Cancer Institute, Boston, MA 02115; [b]Ludwig Center at Dana–Farber/Harvard Cancer Center, Boston, MA 02115; Departments of [c]Pathology and [j]Thoracic/Head and Neck Medical Oncology, University of Texas–M. D. Anderson Cancer Center, Houston, TX 77030; [d]Laboratory of Molecular Cell Biology, Institute of Biochemistry and Cell Biology, Shanghai Institutes for Biological Sciences, Chinese Academy of Sciences, 320 Yue Yang Road, Shanghai 200031, China; [e]Department of Radiology, Beth Israel Deaconess Medical Center, Boston, MA 02115; [f]Department of Pathology, Brigham and Women's Hospital, Boston, MA 02115; [g]Department of Pathology, Harvard Medical School, Boston, MA 02115; [h]Broad Institute of MIT and Harvard, Cambridge, MA 02142; and [i]Department of Pharmacology, Boehringer Ingelheim, A-1120 Vienna, Austria

Edited by Webster K. Cavenee, University of California at San Diego, La Jolla, CA, and approved November 13, 2008 (received for review September 8, 2008)

Mutations in the HER2 kinase domain have been identified in human clinical lung cancer specimens. Here we demonstrate that inducible expression of the most common HER2 mutant (HER2^{YVMA}) in mouse lung epithelium causes invasive adenosquamous carcinomas restricted to proximal and distal bronchioles. Continuous expression of HER2^{YVMA} is essential for tumor maintenance, suggesting a key role for HER2 in lung adenosquamous tumorigenesis. Preclinical studies assessing the in vivo effect of erlotinib, trastuzumab, BIBW2992, and/or rapamycin on HER2^{YVMA} transgenic mice or H1781 xenografts with documented tumor burden revealed that the combination of BIBW2992 and rapamycin is the most effective treatment paradigm causing significant tumor shrinkage. Immunohistochemical analysis of lung tumors treated with BIBW2992 and rapamycin combination revealed decreased phosphorylation levels for proteins in both upstream and downstream arms of MAPK and Akt/mTOR signaling axes, indicating inhibition of these pathways. Based on these findings, clinical testing of the BIBW2992/rapamycin combination in non-small cell lung cancer patients with tumors expressing HER2 mutations is warranted.

lung cancer | murine model

HER2 (erbB-2/neu) is a member of the erbB receptor tyrosine kinase family that also includes EGFR (HER1/erbB-1), HER3 (erbB-3), and HER4 (erbB-4). Whereas these family members usually dimerize upon ligand binding, HER2, for which no ligand is reported, exists mainly in its active conformation. HER2 readily heterodimerizes with other erbB family members and is considered to be the preferred dimerization partner for EGFR, HER3, and HER4 (1). In addition to ligand binding, receptor dimerization can be induced by a high concentration of receptors at the plasma membrane or by kinase domain mutations (2, 3), resulting in receptor activation by the transphosphorylation of tyrosine residues in the C terminus of the respective molecules (4). The phosphorylated residues act as docking sites for an array of downstream signaling molecules activating several biochemical pathways such as the MAPK, the PI3K/Akt/mTOR, the phospholipase C, and the Jak/Stat signaling pathways (2, 3, 5). These signal transduction cascades in concert regulate cellular processes such as proliferation, apoptosis, angiogenesis, migration, adhesion, and differentiation.

Mutations in the HER2 kinase domain have been reported in lung adenocarcinomas at a relatively low frequency of 2–4% (6, 7). Thus far, majority of the HER2 mutations identified in non-small cell lung cancer (NSCLC) samples are in-frame duplications or insertions in a small 8-codon region (codons 774–781 or 775–782) on exon 20. These mutations are analogous to the duplications/insertions in the 9-codon region of exon 20 in *EGFR*, translating to the C terminus of the αC helix in the TK (tyrosine kinase) domain. Based on this similarity, it has been postulated (7) that mutations in HER2 cause a shift in the helical axis that narrows the ATP binding cleft, resulting in both increased TK activity and TK inhibitor sensitivity (8). These HER2 mutations are independent of HER2 receptor overexpression or *KRAS*, *NRAS*, *BRAF*, or *EGFR* mutations (6, 7). However, it remains unclear whether the HER2 mutations detected in human lung cancers are critical for initiation and maintenance of the lung cancer or whether it is a byproduct of a selection process for growth advantage after tumor initiation (9).

To study the in vivo function of the HER2 mutants in lung tumorigenesis, we generated an inducible bitransgenic mouse model that expresses HER2 with an in-frame AYVM insertion at residue M774. This mutant HER2 protein represents 62.5% of all HER2 kinase domain mutations identified, because both M774insAYVM (6) and A775insYVMA (7) lead to identical amino acid changes and will be hereafter referred to as hHER2^{YVMA}. To express the *hHER2^{YVMA}* transgene in the lung type II pneumocytes, we used the established doxycycline-inducible transgenic system using the Clara cell-specific promoter (*CCSP*)-driven reverse tetracycline transactivator (rtTA) protein expressing *CCSP-rtTA* allele (10). MRI was used to document the presence of lung tumors after doxycycline induction and to document tumor volume changes during transgene deinduction or treatment with targeted therapeutics. Here we report that the expression of hHER2^{YVMA} in the lungs drives rapid development of lung carcinomas with adenosquamous features. Deinduction of the hHER2^{YVMA} protein in established lung tumors of transgenic animals caused tumor regression, demonstrating that the mutant HER2 is essential for tumor maintenance. In addition, this newly established transgenic mouse strain was used for treatment studies and could be further used to elucidate mechanisms of drug resistance.

Results

Generation of the *tet-op-hHER2^{YVMA}/CCSP-rtTA* Mouse Cohort. To establish founder mice with inducible expression of the human (h)

Author contributions: S.A.P., U.G., P.G.C., and K.-K.W. designed research; S.A.P., D.L., M.G.R., H.J., L.C., C.L.B., S.Z., K.A.B., S.K., U.G., P.G.C., and F.S. performed research; M.T., G.I.S., H.G., M.M., F.S., and I.I.W. contributed new reagents/analytic tools; S.A.P., T.S., M.G.R., L.R.C., R.F.P., R.T.B., and I.I.W. analyzed data; and S.A.P. and F.S. wrote the paper.

The authors declare no conflict of interest.

This article is a PNAS Direct Submission.

[1]To whom correspondence should be addressed at: Department of Medical Oncology, Lowe Center for Thoracic Oncology, Dana–Farber Cancer Institute, Harvard Medical School, 44 Binney Street, D810, Boston, MA 02115. E-mail: kwong1@partners.org.

This article contains supporting information online at www.pnas.org/cgi/content/full/0808930106/DCSupplemental.

www.pnas.org/cgi/doi/10.1073/pnas.0808930106

HER2^{YVMA} compound mutant, we constructed a 4.75-kb DNA segment consisting of 7 direct repeats of the tetracycline (tet)-operator sequence, followed by hHER2^{YVMA} cDNA and *SV40 poly (A)* [supporting information (SI) Fig. S1*A*]. The construct was injected into FVB/N blastocysts, and transgenic founders were identified by PCR of the human HER2 and *SV40 poly (A)* tail from mouse tail genomic DNA. Three *tet-op-hHER2^{YVMA}* founders identified were crossed to *CCSP-rtTA* mice to generate inducible bitransgenic mouse cohorts harboring both the activator and the responder transgenes (10). Two tightly regulated *hHER2^{YVMA}* founders (designated as HER2 5B and HER2 26) were selected, and the gene copy number from individual founders was determined by quantitative real-time PCR of the *SV40 poly (A)* (Fig. S1*B*).

Expression of mRNA hHER2^{YVMA} Is Tightly Regulated in Lung Epithelium. The inducibility of transgene expression in the lung compartment was evaluated at the RNA level by RT-PCR. The lungs of the bitransgenic *tet-op-hHER2^{YVMA}/CCSP-rtTA* mice for each potential founder were collected at baseline or after 1 week of doxycycline administration. Lungs were also harvested after 2 weeks of doxycycline withdrawal after 8–15 weeks of doxycycline administration. The HER2 mutant transcript was undetectable in lungs from single-transgenic *tet-op-hHER2^{YVMA}* mice with or without doxycycline and the bitransgenic mice without doxycycline treatment (Fig. S1*C* and data not shown). hHER2 transcript was readily detectable in the bitransgenic mice after 1 week of doxycycline administration and was abolished by 2 weeks of doxycycline withdrawal in all animal lines (Fig. S1*C*). Expression levels of the hHER2^{YVMA} transcript in the 2 different founder lines were compared by quantitative PCR from lung mRNA collected after 1 week of doxycycline administration. Interestingly, although HER2 26 had a low copy number (mean = 9 ± 0.9), the expression level was significantly higher than HER2 5B, which had a much higher copy number (mean = 78 ± 12) (Fig. S1 *B* and *D*), implicating that the site of transgene integration into the genome may have an effect on the expression levels (11). To further confirm that mutant HER2 transcripts are inducible and tightly regulated by doxycycline, both RT-PCR and quantitative PCR were performed on lung mRNA, and Western blotting was performed on lung protein samples collected at serial time points after doxycycline administration and withdrawal from founders HER2 26 and/or HER2 5B. Mutant HER2 expression was observed after 1 week of doxycycline administration and was kept at a comparable level throughout the 3- to 8-week period of administration (Fig. S1 *D* and *E*). Doxycycline withdrawal for 3 days was sufficient to extinguish the expression of hHER2^{YVMA} in HER2 26 mice (Fig. S1 *D* and *E*). Furthermore, expression of the transgene was not observed in either line examined after 2 or 12 weeks of doxycycline withdrawal (Fig. S1 *D* and *E*).

Overexpression of the hHER2^{YVMA} Drives Rapid Development of Lung Tumors Displaying Adenosquamous Histology. To examine whether overexpression of hHER2^{YVMA} initiates lung tumorigenesis, bitransgenic *tet-op-hHER2^{YVMA}/CCSP-rtTA* mice were placed on a continuous doxycycline diet at 6 weeks of age and lungs were visualized by serial MRI at 1-week intervals. Mice were also killed at 1-, 2-, 3-, 8-, or 15-week time points for histological examination of the lungs. Tumors were readily identifiable after 1 week of doxycycline diet for founder line HER2 26 whereas HER2 5B took at least 2–3 weeks on doxycycline to develop lesions (Fig. 1*A* and Fig. S2 *A* and *B*). Tumor volume, as defined by MRI, increased after prolonged doxycycline treatment over a 8-week period and a 30-week period for founder lines HER2 26 and HER2 5B, respectively (Fig. S2 *A* and *B*).

Histological examination demonstrated the development of early lesions in airway epithelia after 1–2 weeks of doxycycline treatment. After 3–4 weeks on doxycycline the HER2 26 founder line developed intrabronchial carcinomas in the proximal and distal bronchioloalveolar locations causing premature death by asphyxiation (Fig. 1*A*). The HER2 5B founder line developed similar cancers after 15–18 weeks of doxycycline diet with tumors being generally larger at the time of death. In addition, pleural and chest wall metastatic foci were occasionally observed in the HER2 5B hHER2^{YVMA} mice. The prolonged lifespan in this line (Fig. 1*B*) may have been due to a smaller number of lesions that grow slowly because of low levels of mRNA (Fig. S1*D Right*) and low protein expression (Fig. 1*C*). The apparent discrepancy between protein expression levels observed in off-doxycycline mice for the HER2 26 founder line in Fig. 1*C* and Fig. S1*E* is due to a long exposure used in Fig. 1*C* to visualize protein expression in the HER2 5B founder line.

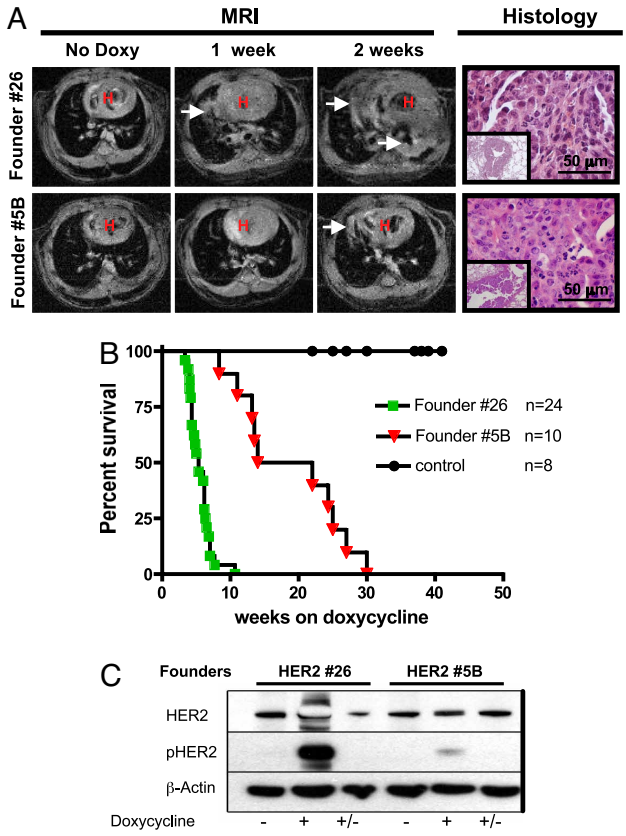

Fig. 1. Expression of hHER2^{YVMA} rapidly induces carcinomas in the bronchioles at 2 different latencies. (*A*) Time course analysis of lung tumorigenesis after doxycycline administration using both MRI and histology. MRI photographs demonstrate rapid increase in tumor volume over a 2-week time span for founder 26 whereas 5B shows only a small lesion at 2 weeks (arrow). H&E-stained high-power and low-power (*Insets*) magnifications show histopathologically similar tumors for 2 founders. Histology was done on moribund mice killed at 4 (founder line 26) or 15 (founder line 5B) weeks. (*B*) Kaplan–Meier survival curves for 2 different founders. 26 has median latency of 5.4 weeks, and 5B has a median latency of 14 weeks. (*C*) Western blots for HER2, phospho-HER2, and β-actin proteins from lungs of 26 and 5B founder line mice that were fed a normal diet (−), 1 week of doxycycline diet (+), and 5 weeks of doxycycline diet followed by 3 days of normal diet (+/−).

Immunohistochemistry (IHC) staining of bronchial tumors with Clara cell secretory protein (CCSP), a specific marker for Clara cells in bronchiolar epithelium, demonstrated CCSP-positive staining in a small subset of bronchial tumor cells (Fig. 2*A*). This is very similar to the staining pattern observed in the bronchiolar tumors of the *tet-op-hEGFR TL/CCSP-rtTA* mice (12). As expected, staining for prosurfactant protein C (SPC), a unique biomarker for type II pneumocytes in the alveoli, was negative in these tumors (Fig. 2*A*). All tumors demonstrated expression of phosphorylated EGFR in a subset of cells, indicating that not all cells have activated EGFR (Fig. 2*A*). The tumors all stained positive with both total and

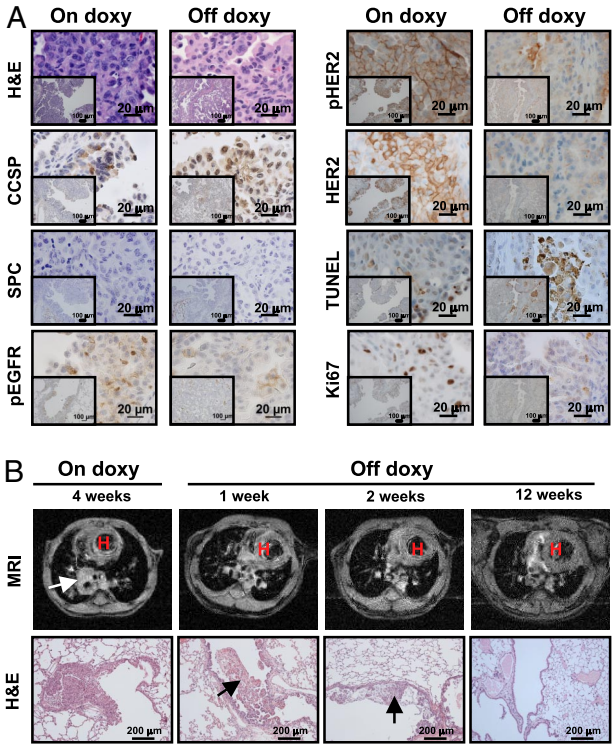

Fig. 2. Tumors depend on hHER2^{YVMA} expression for proliferation but apoptose on hHER2^{YVMA} deinduction. (*A*) Representative photomicrographs of cross-sectional tumors stained with the indicated antibodies from hHER2^{YVMA} founder line 26 on doxycycline diet for 6 weeks (On doxy) and another put on a normal diet for 3 days after 7 weeks of doxycyline diet (Off doxy). At least 3 mice from each founder were analyzed for histology. (*B*) Representative MRI and histology of 1 of 3 mice taken given a normal diet for 1, 2, or 12 weeks after at least 4 weeks of doxycycline. The tumor around a bronchiolar branch identifiable by MRI (arrow) at 4 weeks on doxycycline is not visible after 1, 2, or 12 weeks off diet (H, heart area). By histology, residual tumor (arrow) is seen up to 2 weeks on normal diet but is completely cleared on prolonged administration of normal diet.

phospho-HER2 antibodies (Fig. 2*A*), indicating that the expressed hHER2 mutant is phosphorylated, consistent with a functionally active state. Proliferation was detected by anti-Ki67 staining (Fig. 2*A*), and TUNEL staining was observed only in the periphery of the bronchioloalveolar tumors (Fig. 2*A*).

The hHER2^{YVMA} mouse lung tumors were classified as adenosquamous carcinomas as all tumors observed have a combination of both squamous and glandular differentiation. The squamous feature was confirmed by positive p63 staining, a marker for squamous differentiation (Fig. S3*A*). To further clarify that p63 expression is due to overexpression of HER2, BEAS-2B human lung epithelial cells were stably transduced with vector alone, hHER2^{WT}, or hHER2^{YVMA}. The significantly higher p63 expression levels in both hHER2^{WT} and hHER2^{YVMA} cells (Fig. S3*B*) suggest that HER2 may play an active role in driving squamous differentiation. However, a fraction of mice from founder line HER2 5B were observed to have bronchioloalveolar adenocarcinomas that did not stain positive for p63 (Table S1 and data not shown). Taken together, these data show that, when overexpressed, hHER2^{YVMA} is a potent initiator of lung adenosquamous carcinoma in murine airways.

Expression of the hHER2^{YVMA} Mutant Is Essential for Tumor Maintenance. To assess tumor dependence on hHER2^{YVMA} signaling, mice carrying established tumors (3–4 weeks) were taken off the doxycycline diet for 3 days, and the lungs were sectioned and stained for CCSP, SPC, phospho-EGFR, and total and phospho-HER2 (Fig. 2*A*). Immunostaining for phospho-EGFR, total HER2, and phospho-HER2 was decreased after 72 h, implying that tumors are driven by and depend on hHER2^{YVMA} for their survival. SPC staining was negative regardless of doxycycline status. We also observed an increase in TUNEL staining (72 h) after doxycycline withdrawal, indicating an increase in apoptosis (Fig. 2*A*) as well as a decrease in Ki67 immunostaining consistent with decreased proliferation of cancer cells (Fig. 2*A*).

With prolonged doxycycline withdrawal (1, 2, or 12 weeks), hHER2^{YVMA}-driven lung tumors regressed completely as assessed by MRI (Fig. 2*B*). Examination of lungs from tumor-bearing mice after 1- or 2-week doxycycline withdrawal showed the presence of residual tumors in some mice (Fig. 2*B Lower*). However, no tumors were found in airways after 12 weeks of doxycycline withdrawal in >5 other tumor-bearing mice examined (Fig. 2*B* and Fig. S2*C*).

hHER2^{YVMA}-Driven Lung Tumors Respond Differentially to Erlotinib, Trastuzumab, BIBW2992, Rapamycin, and BIBW2992/Rapamycin Treatment. To investigate the antitumor activity of various erbB-targeted therapies we serially imaged hHER2^{YVMA} transgenic mice with established tumors after 2–4 weeks of doxycycline treatment. At least 5 bitransgenic *tet-op-hHER2^{YVMA}/CCSP-rtTA* mice with a minimum of 25% (of total lung) tumor burden as determined by MRI were assigned for each therapeutic study. Mice were kept on continuous doxycycline administration during the entire drug treatment period of 2 or more weeks.

Placebo mice that were administered drug solvent either orally or i.p. showed substantial tumor growth over the 2-week period (Fig. 3 *A* and *B*). Erlotinib, a reversible EGFR inhibitor (13), was administered at a daily dose of 50 mg/kg. These mice displayed treatment insensitivity with 33–119% tumor growth (mean = 72.94 ± 17% relative tumor volume; Fig. 3*B*). Histological analyses of the lungs from treated mice did not reveal any treatment effect when comparing erlotinib- with placebo-treated control mice (Fig. 3*A*). Mice treated with trastuzumab, a humanized monoclonal anti-HER2 antibody injected biweekly i.p. at 100 mg/kg (14), showed, on average, a favorable tumor regression of 13.59 ± 10.89% (Fig. 3*B*). However, histological analyses showed limited treatment effect in these mice (Fig. 3*A*). Next we examined the effect of BIBW2992, an irreversible dual EGFR/HER2 inhibitor, because a similar TKI had been shown to be highly effective against Ba/F3 cells expressing mutant HER2 and H1781 cell lines harboring another activating HER2 mutation (HER2$^{G776insV_G/C}$) (15). Daily oral administration of 20 mg/kg BIBW2992 as a single agent caused an average regression rate of 36.8 ± 6.5% by MRI (Fig. 3*B*). In addition to statistically significant reduction in tumor volume (P = 0.003), histological analysis demonstrated a pronounced treatment effect when compared with placebo or erlotinib treatment (Fig. 3*A*).

Because HER2 mutations were shown to be potent activators of the Akt/mTOR pathway (9) and because rapamycin proved to be effective in inhibiting EGFR$^{L858R\ T790M}$ lung alveolar and bronchiolar tumors when used in combination with the irreversible inhibitor BIBW2992 (16) or another irreversible TK inhibitor, HKI-272 (12), we investigated the antitumor activity of rapamycin as a single agent or in combination with BIBW2992. Rapamycin administered via i.p. injection at 2 mg/kg every other day caused on average a 24.7 ± 10.9% tumor regression by MRI (P = 0.0011 compared with erlotinib; Fig. 3*B*). Histological examination showed focal changes consistent with treatment effect in the lung tumors (Fig. 3*A*). Combining rapamycin given every other day (2 mg/kg, i.p. injection) with BIBW2992 given daily (20 mg/kg, oral gavage) caused a significant reduction (P = 0.0004 compared with erlotinib) in tumor volume (50.1 ± 27.4%) after a 2-week treatment period (Fig. 3*B*). Histological examination of the tumors showed decreased cellularity, increased fibrosis, and necrosis, thus confirming the MRI findings (Fig. 3*A*). Interestingly, the superiority of the BIBW2992/rapamycin combination treatment as compared with single-agent treatments was also observed in the H1781 NSCLC cell

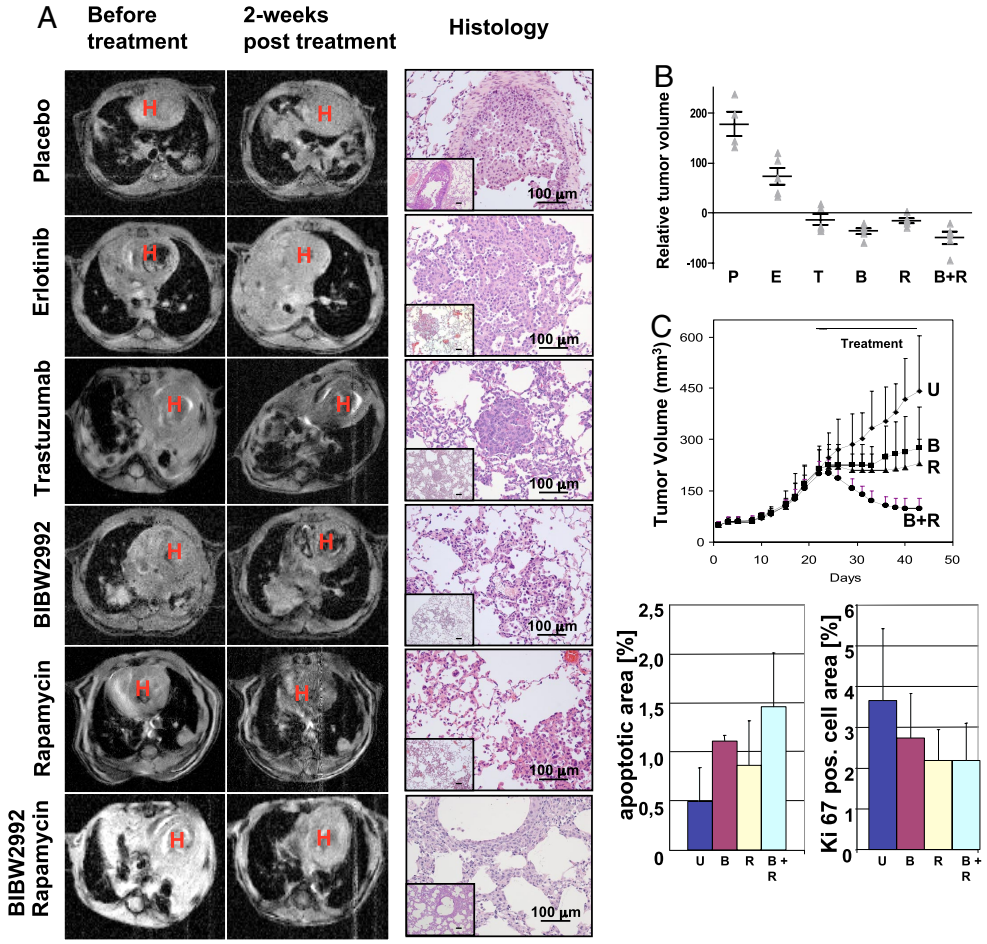

Fig. 3. Differential response of adenosquamous tumors driven by hHER2^{YVMA} expression to 2-week treatment with erlotinib, trastuzumab, BIBW2992, rapamycin, or BIBW2992/rapamycin combination. (*A*) MRI, histology, and relative tumor volume of bitransgenic *tet-op-hHER2^{YVMA}/CCSP-rtTA* mice treated with empty vehicle, erlotinib at 50 mg/kg, trastuzumab at 100 mg/kg twice per week, BIBW2992 at 20 mg/kg, rapamycin at 2 mg/kg, or both BIBW2992 at 20 mg/kg orally and rapamycin at 2 mg/kg every other day by i.p. injection. The mice were imaged with MRI before and after 2 weeks of treatment. Representative imaging is shown for MRI (H, heart area). Histology is from the same mice shown by MRI. The bar in inset is 100 μm. (*B*) Dot plot diagram expressed with mean ± SEM illustrates the relative tumor regression measured by MRI before and after 2 weeks of treatment for 4–5 different mice. Statistical analyses were performed by using Student's 2-tailed *t* test. (*C*) Response of established H1781 NSCLC tumors to BIBW2992, rapamycin, or a combination thereof—BIBW2992 was administered daily p.o. at 20 mg/kg (■) and rapamycin i.p. at 2 mg/kg (▲). In the combination arm (●) both drugs were given concomitantly at the same doses and regimen as the single agents. (♦), growth of untreated tumors. Each group comprised 7 animals; data points are averages, and error bars represent standard deviations. Apoptosis and proliferation assessed by cCK18 staining and Ki-67, respectively, were quantified from 4 tumor fields of 2 different tumors and graphed as a percentage of the total area (*Lower*). P, placebo; U, untreated; E, erlotinib; T, trastuzumab; B, BIBW2992; R, rapamycin.

line (Fig. S4). Indeed, the BIBW2992/rapamycin combination treatment of mice carrying large (≈200-mm^3) H1781 tumors resulted in significant tumor regressions in all treated animals whereas single agents delayed or stopped tumor growth (Fig. 3*C*). To investigate the additive effect of the combination drug treatment IHC was carried out on these tumors to monitor apoptosis, necrosis, and proliferation. We found a 2-fold increase in apoptosis marker (as assessed by cCK18 staining) upon combination therapy, a marked increase in necrosis, and decreased proliferation (as assessed by Ki-67 staining) in all treatment groups when compared with controls (Fig. 3*C* and Fig. S5).

To investigate the treatment effects on signaling pathways and confirm "on-target" effects of the various drugs, mice bearing hHER2^{YVMA}-driven tumors were treated with trastuzumab, BIBW2992, rapamycin, or the combination of BIBW2992 and rapamycin for 72 h, and fixed lungs were IHC-stained for signaling molecules including total HER2, phospho-HER2, phospho-EGFR, phospho-MAPK, phospho-Akt, and phospho-S6. Trastuzumab effectively decreased phosphorylated membranous but not cytoplasmic HER2 whereas BIBW2992 decreased both total and phospho-HER2 in both membrane and cytoplasmic locations (Fig. 4 and data not shown). Downstream signaling of erbB family members such as Akt and MAPK were also inhibited more effectively by BIBW2992 compared with trastuzumab. Phospho-S6 was not altered dramatically except on rapamycin mono or dual therapy with BIBW2992. As expected, rapamycin alone did not significantly alter HER2, EGFR, Akt, and MAPK phosphorylation levels. Combination of BIBW2992 and rapamycin dramatically decreased phospho-S6 levels compared with BIBW2992 alone (Fig. 4). These data demonstrate that the combination of BIBW2992 and rapamycin is the most effective regimen at inhibiting both upstream and downstream signaling of both the erbB/PI3K/mTOR and the MAPK signaling pathways.

Discussion

The role of HER2 in cancer is complex and involves other erbB family members, their ligands, and a multitude of downstream signaling molecules. In the present study we describe an inducible in vivo model of murine lung carcinoma driven by hHER2^{YVMA} yielding a unique adenosquamous histology. Using genetically

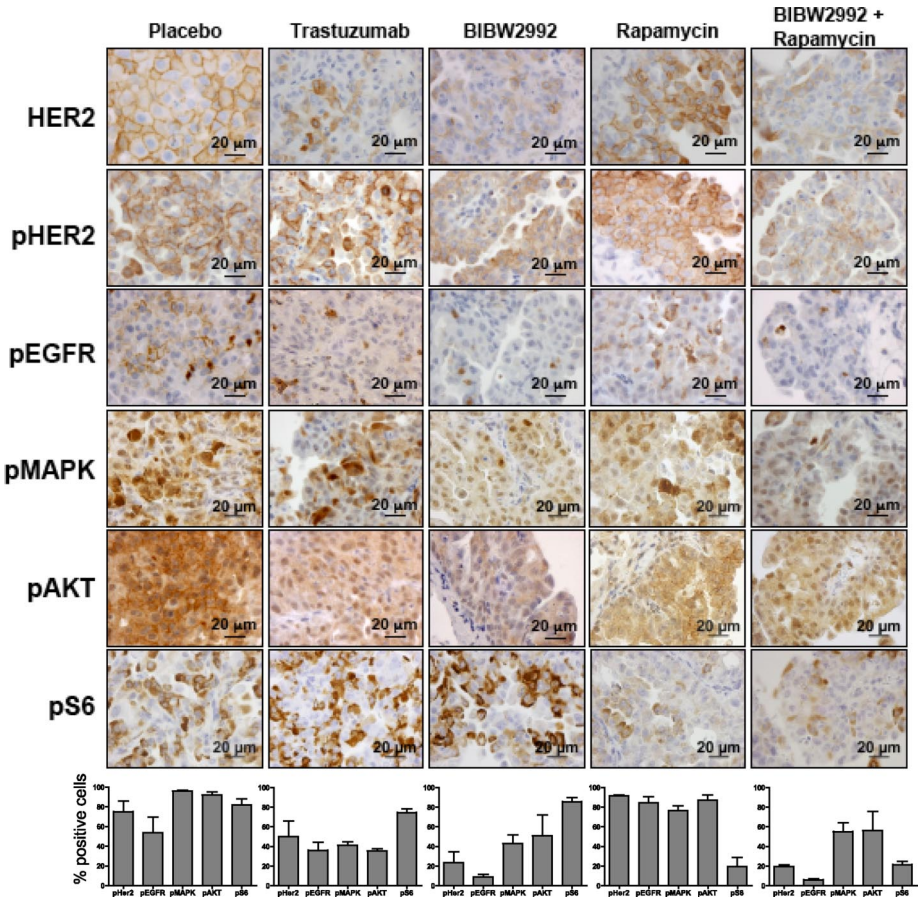

Fig. 4. Immunohistochemical assessment reveals that phosphorylation of HER2 and downstream signaling molecules are most decreased with combination of BIBW2992 and rapamycin. Bitransgenic *tet-op-hHER2^{YVMA}/CCSP-rtTA* mice were treated with trastuzumab, BIBW2992, rapamycin, or the combination of BIBW2992 and rapamycin therapy for 72 h, and lung sections were then stained with antibodies recognizing phospho-HER2, phospho-EGFR, phospho-Akt, phospho-MAPK, and phospho-S6. IHC photographs are representative fields from duplicate animals in each group. The bar in each photomicrograph is 20 μm. Quantitative analyses of 6 different high-power tumor images from 2 mice are presented as percent positive cells in a tumor area in the bar graphs.

engineered hHER2^{YVMA} mice and standard xenograft models as platforms for testing different therapeutics, we identified the BIBW2992/rapamycin combination as a potential treatment modality that may be used for clinical testing in patients whose tumors harbor *hHER2^{YVMA}* mutations.

Targeted expression of the HER2 kinase domain duplication/insertion YVMA mutant in the murine pulmonary tissue is strongly oncogenic, driving rapid tumor proliferation mainly in proximal and distal airway epithelia of most mice. These HER2 mutant-driven bronchiolar lung carcinomas have a unique histology with both glandular and squamous differentiation within most tumors observed. Therefore, these bronchioloalveolar tumors were classified as adenosquamous carcinomas. The peripheral bronchioloalveolar adenocarcinoma along with airway adenosquamous carcinomas observed in a small percentage of mice from founder line HER2 5B may have been due to the lower expression of hHER2^{YVMA} in this group (Table S1 and Fig. S1). These results demonstrate that high expression of HER2 can drive adenosquamous carcinomas in murine airways.

The striking histologic and radiologic (17) phenotype similarity of hHER2^{YVMA}-driven murine carcinoma to human bronchogenic adenosquamous carcinomas prompted us to examine HER2 expression in human lung adenosquamous carcinomas (fully described in *SI Text*). We found that a high percentage (67%) of human adenosquamous lung cancers had increased membranous HER2 staining (Table S2 and Fig. S6). This is significantly higher than HER2-positive staining reported for adenocarcinomas, squamous cell carcinomas, or large-cell carcinomas of the lung (Table S3) (18). Although none of the human adenosquamous tumors we analyzed carried a *HER2* mutation, membranous HER2 protein localization or HER2 overexpression may activate signaling molecules analogous to mutant HER2 because overexpression of wild-type human HER2 is also transforming in NIH 3T3 cells and mammary epithelial cells (19, 20). Thus, the adenosquamous differentiation that we observed in carcinomas from *tet-op-hHER2^{YVMA}/CCSP-rtTA* mice may be analogous to the human lung adenosquamous carcinomas where HER2 is highly expressed. The bronchioloalveolar adenocarcinoma observed in the hHER2^{YVMA}-expressing 5B founder line may be due to the decreased expression levels observed in these mice similar to adenocarcinomas in human patients with elevated HER2. More HER2-expressing human samples may need to be studied to confirm this in a human context. Of note, this adenosquamous phenotype may be restricted to the pulmonary tissue because it is not a common feature of HER2-positive human breast tumors.

In our study, deinduction of hHER2^{YVMA} expression caused regression of the induced lung carcinomas, thus identifying HER2^{YVMA} as a possible therapeutic target for a subset of NSCLC patients. BIBW2992 was the most effective single agent when compared with erlotinib, trastuzumab, or rapamycin in these de novo hHER2^{YVMA}-driven lung tumors and resulted in an average 37% tumor regression (range: 20% to 59%). The tumor growth delay seen in erlotinib-treated mice compared with placebo may be a result of competition between erlotinib inhibition and HER2^{YVMA} transactivation of EGFR. The mechanistic reason for the relatively low trastuzumab effect seen in the hHER2^{YVMA}-driven lung tumors is less clear because a *HER2* mutant human cell line (H1781) is relatively sensitive to trastuzumab (9). A possible explanation may be that trastuzumab is effective at inhibiting phosphorylation of membranous HER2 but unable to inhibit intracellular HER2 protein signaling associated with Golgi, endoplasmic reticulum, and other transport vesicles. This is in line with clinical findings showing that trastuzumab does not provide significant survival advantage when combined with first-line chemother-

apy in NSCLC patients with or without stratification for HER2 overexpression (21, 22). These results suggest that trastuzumab may be less effective in inhibiting the more potent signaling transduced by the activating YVMA insertion mutation of *HER2* (9) under in vivo conditions, thus illustrating the importance of using a more "humanized" model for drug testing.

Mutant HER2 has been documented to be a strong driver of Akt phosphorylation and activation (9). Furthermore, inhibition of mTOR, a signaling molecule downstream of the Akt, along with EGFR inhibition using BIBW 2992 or HKI-272 was shown to be most effective against $EGFR^{L858R\ T790M}$ mutant-driven murine lung tumors (12, 16). We therefore used a similar strategy on the $hHER2^{YVMA}$- and $HER2^{G776insV\ G/C}$-driven carcinomas by using BIBW2992 and rapamycin. Interestingly, rapamycin single therapy was observed to be more effective in the $hHER2^{YVMA}$ than the $EGFR^{L858R\ T790M}$ murine model. This implies that mutant HER2 may be more dependent on the Akt/mTOR pathway for oncogenesis than $EGFR^{L858R\ T790M}$ possibly through HER3 activation. However, the most effective treatment regimen was combination of BIBW2992/rapamycin, which caused significant tumor shrinkage of the recalcitrant adenosquamous carcinomas in the transgenic model and in the H1781 xenograft model. Thus, combination of an irreversible TK inhibitor with an mTOR inhibitor such as rapamycin, temsirolimus, or everolimus may be of benefit to patients with HER2-expressing tumors. These preclinical findings provide a sound rationale for the clinical testing of the BIBW2992/rapamycin combination treatment modality in cancer patients with $hHER2^{YVMA}$-driven or HER2-overexpressing lung carcinomas. Finally, the genetic adenosquamous lung carcinoma described here will serve as an ideal platform to effectively characterize the pathogenesis and responsiveness to therapeutics of this rare lung cancer type.

Experimental Procedures

Generation of the *tet-op-hHER2^{YVMA}/CCSP-rtTA* Mouse Cohort. To generate the transgenic mouse lines with doxycycline-inducible expression of the human *HER2* insertion mutant, the transgene DNA construct was subcloned into pTRE-hyg (Clontech) as described in *SI Text*. All mice were housed in a pathogen-free environment at the Harvard School of Public Health and were handled in strict accordance with Good Animal Practice as defined by the Office of Laboratory Animal Welfare, and all animal work was done with Dana–Farber Cancer Institute Institutional Animal Care and Use Committee approval.

RT-PCR and Quantitative PCR. Transgene copy numbers were determined by real-time PCR carried out on tail and spleen DNA. Total RNA samples were prepared as previously described (12, 13) and retrotranscribed into first-strand cDNA using the SuperScript First Strand Synthesis System following the manufacturer's protocol (Invitrogen). Quantitative PCR was performed as described in ref. 12.

Immunohistochemistry and TUNEL Assays. Mice were killed, and right lungs were fixed in 10% formalin, embedded in paraffin, and sectioned at 5 μm as described previously (12). Left lungs were frozen for RNA or protein assays. IHC was performed as described in ref. 12 using total HER2 (A0485; DAKO) and phospho-HER2 (Cell Signaling Technology), SPC (Chemicon), CCSP (Santa Cruz Biotechnology), and p63 (DAKO). Apoptosis was measured by TUNEL assay (ApopTag kit; Chemicon). Ki-67 antibody (Vector Laboratories) was used to evaluate cell proliferation.

Targeted Therapy. Mice were put on continuous doxycycline diets at 6 weeks of age for >4 weeks, and bitransgenic mice were subjected to MRI to document lung tumor burden. After initial imaging, either erlotinib (bought commercially) at 50 mg/kg or BIBW2992 (Boehringer Ingelheim) at 20 mg/kg formulated in 0.5% methocellulose–0.4% polysorbate 80 (Tween 80) were administrated daily by gavage. Trastuzumab (from the Dana–Farber Cancer Institute pharmacy) was diluted in saline and injected every 3 days i.p. at 100 mg/kg. Rapamycin (LC Laboratories) formulated in 5% PEG400 and 5% Tween 80 was administered by i.p. injection at 2 mg/kg every other day. The mice were imaged before, during, and after treatment by MRI to determine the reduction in tumor volume weekly during the respective treatments and then killed for further histological and biochemical studies. Treatments were continued for 2 or 3 weeks to induce maximal tumor response. Erlotinib treatment was stopped after 2 weeks because of increasing tumor burden. Littermates were used as control for all treatment groups.

MRI Scanning and Tumor Volume Measurement. MRI scanning and tumor volume measurement were done as described previously (12, 13). Statistical analyses were performed by the using unpaired 2-tailed Student *t* test. *P* values of <0.05 were considered significant.

In Vivo Xenograft Experiments. Five- to 6-week-old female BomTac:NMRI-Foxn1^{nu} mice were maintained under specific pathogen-free conditions. All experiments complied with the Declaration of Helsinki and European Policy Legislations [Federation of European Laboratory Animal Science Associations (FELASA) and Die Gesellschaft für Versuchstierkunde (GV-SOLAS)] on the care and use of laboratory animals. After acclimatization mice were inoculated s.c. into the right flank with 5×10^6 H1781 NSCLC cells using Matrigel and treated as detailed in *SI Text*. IHC carried out on tumor sections are also detailed in *SI Text*.

ACKNOWLEDGMENTS. We thank Dr. Jeffrey Whitsett (Cincinnati Children's Hospital Medical Center, Cincinnati, OH) for providing the CCSP-rtTA transgenic mice. We also thank Eva Strauss, Astrid Jeschko, Stefan Fischer, Christine Lam, and Mei Zheng for technical support. This work was supported by the Cecily and Robert Harris Foundation (K.-K.W.); the Joan Scarangello Foundation to Conquer Lung Cancer (K.-K.W.); the Flight Attendant Medical Research Institute (K.-K.W.); and National Institutes of Health Grants R01 AG2400401 (to K.-K.W.), R01 CA122794 (to K.-K.W.), P20 CA90578 (to K.-K.W., G.I.S., and L.R.C.), and R01 CA90687 (to G.I.S.). T.S. is supported by a Career Development Award as part of the Dana–Farber/Harvard Cancer Center Specialized Program of Research Excellence in Lung Cancer and National Institutes of Health Grant P20 CA90578.

1. Graus-Porta D, Beerli RR, Daly JM, Hynes NE (1997) ErbB-2, the preferred heterodimerization partner of all ErbB receptors, is a mediator of lateral signaling. *EMBO J* 16:1647–1655.
2. Ono M, Kuwano M (2006) Molecular mechanisms of epidermal growth factor receptor (EGFR) activation and response to gefitinib and other EGFR-targeting drugs. *Clin Cancer Res* 12:7242–7251.
3. Yarden Y, Sliwkowski MX (2001) Untangling the ErbB signalling network. *Nat Rev Mol Cell Biol* 2:127–137.
4. Garrett TP, *et al.* (2003) The crystal structure of a truncated ErbB2 ectodomain reveals an active conformation, poised to interact with other ErbB receptors. *Mol Cell* 11:495–505.
5. Engelman JA, Cantley LC (2006) The role of the ErbB family members in non-small cell lung cancers sensitive to epidermal growth factor receptor kinase inhibitors. *Clin Cancer Res* 12:4372s–4376s.
6. Stephens P, *et al.* (2004) Lung cancer: Intragenic ERBB2 kinase mutations in tumours. *Nature* 431:525–526.
7. Shigematsu H, *et al.* (2005) Somatic mutations of the HER2 kinase domain in lung adenocarcinomas. *Cancer Res* 65:1642–1646.
8. Gazdar AF, Shigematsu H, Herz J, Minna JD (2004) Mutations and addiction to EGFR: The Achilles 'heal' of lung cancers? *Trends Mol Med* 10:481–486.
9. Wang SE, *et al.* (2006) HER2 kinase domain mutation results in constitutive phosphorylation and activation of HER2 and EGFR and resistance to EGFR tyrosine kinase inhibitors. *Cancer Cell* 10:25–38.
10. Fisher GH, *et al.* (2001) Induction and apoptotic regression of lung adenocarcinomas by regulation of a K-Ras transgene in the presence and absence of tumor suppressor genes. *Genes Dev* 15:3249–3262.
11. Jordan A, Defechereux P, Verdin E (2001) The site of HIV-1 integration in the human genome determines basal transcriptional activity and response to Tat transactivation. *EMBO J* 20:1726–1738.
12. Li D, *et al.* (2007) Bronchial and peripheral murine lung carcinomas induced by T790M-L858R mutant EGFR respond to HKI-272 and rapamycin combination therapy. *Cancer Cell* 12:81–93.
13. Ji H, *et al.* (2006) The impact of human EGFR kinase domain mutations on lung tumorigenesis and in vivo sensitivity to EGFR-targeted therapies. *Cancer Cell* 9:485–495.
14. Azzoli CG, Krug LM, Miller VA, Kris MG, Mass R (2002) Trastuzumab in the treatment of non-small cell lung cancer. *Semin Oncol* 29:59–65.
15. Minami Y, *et al.* (2007) The major lung cancer-derived mutants of ERBB2 are oncogenic and are associated with sensitivity to the irreversible EGFR/ERBB2 inhibitor HKI-272. *Oncogene* 26:5023–5027.
16. Li D, *et al.* (2008) BIBW2992, an irreversible EGFR/HER2 inhibitor highly effective in preclinical lung cancer models. *Oncogene* 27:4702–4711.
17. Kazerooni EA, Bhalla M, Shepard JA, McLoud TC (1994) Adenosquamous carcinoma of the lung: Radiologic appearance. *Am J Roentgenol* 163:301–306.
18. Nakamura H, Kawasaki N, Taguchi M, Kabasawa K (2005) Association of HER-2 overexpression with prognosis in nonsmall cell lung carcinoma: A metaanalysis. *Cancer* 103:1865–1873.
19. Kokai Y, *et al.* (1989) Synergistic interaction of p185c-neu and the EGF receptor leads to transformation of rodent fibroblasts. *Cell* 58:287–292.
20. Pierce JH, *et al.* (1991) Oncogenic potential of erbB-2 in human mammary epithelial cells. *Oncogene* 6:1189–1194.
21. Gatzemeier U, *et al.* (2004) Randomized phase II trial of gemcitabine-cisplatin with or without trastuzumab in HER2-positive non-small-cell lung cancer. *Ann Oncol* 15:19–27.
22. Hirsch FR, Langer CJ (2004) The role of HER2/neu expression and trastuzumab in non-small cell lung cancer. *Semin Oncol* 31:75–82.